

Bio-inspired recognition of dopamine versus ascorbic acid

T. Mary Vergheese, Sheela Berchmans *

Central Electrochemical Research Institute (CECRI), Karaikudi 630 006, Tamil Nadu, India

Received 8 January 2004; received in revised form 1 March 2004; accepted 15 March 2004

Available online 2 July 2004

Abstract

The concept of a bio-inspired oxidation reaction is used along with self-assembled monolayers for the selective recognition of dopamine over ascorbic acid (AA) in this work. Self-assembled monolayers with negatively charged terminal groups are manipulated for selective sensing of dopamine (DA). It is observed that the recognition sensitivity is increased in the mixed monolayer configuration, and this is increased further when copper ions are included in the SAM matrix by chelation. Monolayers of mercaptoundecanoic acid (MUA) and mercaptobenzothiazole (MBT) and mixed monolayers with decanethiol (DT) (viz., DT+MUA and DT+MBT) are used in the present investigations. Good selectivity is observed in the case of the Au/MUA, Au/MUA/Cu²⁺ and Au/(DT+MUA)/Cu²⁺ films. The oxidation of AA and DA occurs as two separate peaks in these configurations and hence better recognition is achieved.

© 2004 Elsevier B.V. All rights reserved.

Keywords: Dopamine; Ascorbic acid; Self assembled monolayers; Bio-inspiration; Voltammetry

1. Introduction

Researchers customarily try to explore the efficiency of highly expensive catalytic materials such as transition metals like Pt, Pd, Rh or Ru for challenging organic reactions as in the controlled oxidation of C–H bonds [1]. When one tries to find out how Mother Nature performs these types of reactions, it is surprisingly observed that commonly available metals like iron, zinc and copper are involved in the enzyme catalysed biochemical reactions [2]. With this in mind we have attempted to explore the catalytic oxidation of dopamine (DA) initiated by copper, as the basis of the recognition of DA using self-assembled monolayers. The genesis of the idea of using copper as the catalyst arises from the following facts observed in biological systems. Tyrosinase, a di-nuclear copper(II)-containing protein is found to orthohydroxylate monophenols and further oxidizes *o*-diphenol to an *o*-quinone [3,4]. DA β-monooxygenase [5] is an enzyme based on copper which catalyses the

conversion of DA into norepinephrine [6–8]. Another metalloenzyme based on cupric ions is ascorbate oxidase in which the copper is bound to the imidazole groups by the nitrogen and to cysteine residues by the sulphur in the enzyme active sites [9].

The concept of a bio-inspired oxidation reaction is used along with self-assembled monolayers for the selective recognition of DA over ascorbic acid (AA). DA [10–17] plays an important physiological role as an extra-cellular chemical messenger. Parkinson's disease is a degenerative brain disorder with symptoms that include tremor, rigid posture, slow movements, etc. and it arises due to the lack of DA in brain fluids [18,19]. Because DA and the other neurotransmitters like catecholamines are easily oxidized, electrochemical methods based on anodic oxidation have generally been used to monitor their concentrations. Electrochemical determination of DA is complicated by the coexistence of many interfering compounds. Among them AA is of particular importance because this species is oxidized at a potential close to that of DA and it occurs in larger concentrations compared to DA [20–23]. Another worrying issue is the electrocatalytic oxidation of DA by AA [24,25]. Namely, oxidized DA, i.e. DA *o*-quinone is chemically

* Corresponding author. Tel.: +91-45652-27551; fax: +91-45652-27771.

E-mail address: berchmansheela@rediffmail.com (S. Berchmans).

reduced by AA. Hence the oxidation current of DA will be altered. To increase selectivity, many different methods of electrode pretreatment and electrochemical modification have been reported [26–33].

One of the promising approaches is the use of self-assembled monolayers. The use of self-assembled monolayers for a variety of applications such as sensors, catalysis, electrochemical rectification, electrode kinetics, etc., has already been established in our laboratory [34–40].

The recognition of DA over AA using self-assembled monolayers, which are negatively charged at neutral pH, is the basis of the present investigation. The amine group of DA is positively charged ($pK_b = 8.87$) whereas the hydroxyl group next to the carbonyl group of AA is negatively charged at neutral pH ($pK_a = 4.1$) [41–43]. DA, being positively charged, is attracted by the negatively charged monolayer and AA, being negatively charged, is repelled away from the monolayer. This forms the basis of the separation of these two compounds.

The compounds chosen for the formation of SAMs are mercaptobenzothiazole (MBT), mercaptoundecanoic acid (MUA) and decanethiol (DT) (Scheme 1). Monolayers and mixed monolayers are formed. MBT has been chosen because it is found that imidazoles are the building block unit of copper-containing enzymes like ascorbate oxidase. MBT is known to complex Cu^{2+} ions [44] and MBT, which is a derivative of thiazole, contains an aromatic ring fused with a thiazole ring through which the monolayer is formed [45]. The pK_a of 2-MBT is 6.93 at 20 °C and it exists in two forms, namely the thione form and the thiol form [45–47]. In an acid medium MBT is present in the thione form [48,49]. In a basic medium it exists in the thiol ion form (MBT^-) [45]. A combination of surface enhanced Raman spectroscopy (SERS) and ab initio molecular orbital calculations [50] suggest that MBT monolayers on gold have

higher thermal stability when compared to other alkane thiol monolayers, MBT adsorbs with its molecular plane perpendicular to the surface of gold, in the thione form [51]. Our experience with XPS experiments on mercaptobenzimidazoles has also indicated that Cu is chelated to the imidazole unit and it is also well known that mercaptobenzimidazoles and MBTs are structurally related heterocyclic thiols [52]. MUA has been chosen, as it is known to complex Cu^{2+} ions [53]. DT is chosen to form a mixed monolayer with MBT and MUA. The presence of DT increases the structural integrity of the monolayers and the monolayers become compact and impervious. Eight different types of electrode configurations are used in the investigations: (1) Au/MBT, (2) Au/MUA, (3) Au/(DT+MBT), (4) Au/(DT+MUA), (5) Au/MBT/ Cu^{2+} , (6) Au/MUA/ Cu^{2+} , (7) Au/(DT+MBT)/ Cu^{2+} and (8) Au/(DT+MUA)/ Cu^{2+} . The influence of each configuration in the selective recognition of DA is described in detail in this paper.

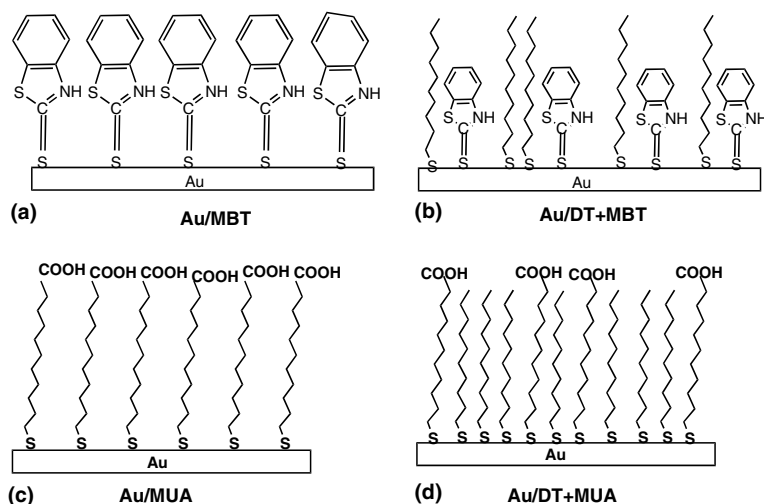
2. Experimental

2.1. Chemicals used

Mercaptobenzothiazole was purchased from Fluka. MUA and DT were purchased from Aldrich. 3-Hydroxytyramine hydrochloride (DA) was purchased from Acros Organics and AA was purchased from Indian Drugs and Pharmaceuticals Ltd. All the other reagents used were of Analar Grade.

2.2. Apparatus

All the cyclic voltammetric experiments were carried out using a Wenking LB 75L potentiostat, a Wenking



Scheme 1. Different SAMs chosen for investigation: (a) Au/MBT, (b) Au/(DT+MBT), (c) Au/MUA and (d) Au/(DT+MUA).

(Model VSG 72) voltage scan generator and a Rikadenki X–Y recorder. Experiments were conducted using a three-electrode cell.

2.3. Electrodes

A gold (BAS) electrode of area 0.07 cm^2 was used as the working electrode. Platinum foil was used as the counter electrode and mercury-mercurous sulphate (MMS, $1 \text{ M H}_2\text{SO}_4$) was used as the reference electrode.

All the reactions were carried out in pH 7.62 phosphate buffer. 10 mM DA , 100 mM and 1 M AA and 5 mM CuSO_4 were used as stock solutions for the recognition experiments. All the solutions were prepared using triply distilled water.

2.4. Standardization of gold electrodes

The gold electrodes, of 0.07 cm^2 area, were cleaned using alumina slurry on emery papers of grade 3, 4 and 5. The cleaned electrodes were washed in triply distilled water and cycled in $0.5 \text{ M H}_2\text{SO}_4$, in the potential range of -0.4 V to $+1.2 \text{ V}$. The cycling was continued till a reproducible voltammogram showing the presence of gold oxide formation and reduction was obtained. The electrode was further standardized using a redox species of $[\text{Fe}(\text{CN})_6]^{4-/3-}$ in $0.5 \text{ M H}_2\text{SO}_4$ in the potential range of -0.4 V to $+0.2 \text{ V}$. A ΔE_p value of 60 mV was considered as the criterion for a standardized electrode. Once the electrodes were standardized they were used for further modification.

2.5. Modification of the electrode

Au/MBT modified electrode: The standardized electrode was dipped in 1 mM MBT dissolved in acetone and left to stand overnight. The modified electrode was washed with acetone and used for further experiments.

Au/MUA modified electrode: The standardized electrode was dipped in a 1 mM ethanolic solution of MUA overnight. The modified electrode was washed with ethanol and used for further experiments.

Au/DT+MBT modified electrode: The standardized electrode was dipped in DT for 1 h, rinsed with ethanol and then dipped in 1 mM MBT dissolved in acetone for 3 h. The electrode was washed with acetone and used for further experiments.

Au/DT+MUA modified electrode: The standardized electrode was dipped in DT for 1 h, rinsed with ethanol and then dipped in an ethanolic solution of MUA for 3 h. The modified electrode was washed with ethanol and used for further experiments.

Preconcentration of Cu^{2+} on the above electrode configurations: Cu^{2+} was preconcentrated chemically by immersing the Au/SAM modified electrode in the buffer solution containing Cu^{2+} ions followed by electro-

chemical reduction similarly to the procedure described elsewhere [40]. In brief, the Au/SAM modified electrode was immersed in the Cu^{2+} solution for 10 min. After that the electrode was washed thoroughly with water and then electrochemically reduced at a negative potential of -0.7 V vs. $\text{Hg}|\text{Hg}_2\text{SO}_4$ for 10 min, after which it was then used for the experiments.

3. Results and discussion

3.1. Bare gold electrode

Fig. 1 represents the cyclic voltammetric response obtained for the bare gold electrode in (a) 1 mM of DA in phosphate buffer and (b) 1 mM of AA in phosphate buffer at a scan rate of 50 mV/s . It is observed from the figure that DA is oxidized at the bare gold electrode at a potential of 130 mV at $v = 50 \text{ mV/s}$ and AA is irreversibly oxidized at a potential of -115 mV . The electrochemical oxidation of the DA and AA corresponds to a two-electron deprotonation process (Scheme 2). The less positive peak potential for AA as compared to DA at the bare electrode and the fact that the concentration of AA is several orders of magnitude higher than DA in a biological environment results in low selectivity for detection of DA at bare electrode. Figs. 2 and 3 show CVs for the two films Au/(DT+MUA) and Au/MUA/ Cu^{2+} indicating the analytical utility of the films studied for sensing DA. The figures clearly show that the DA

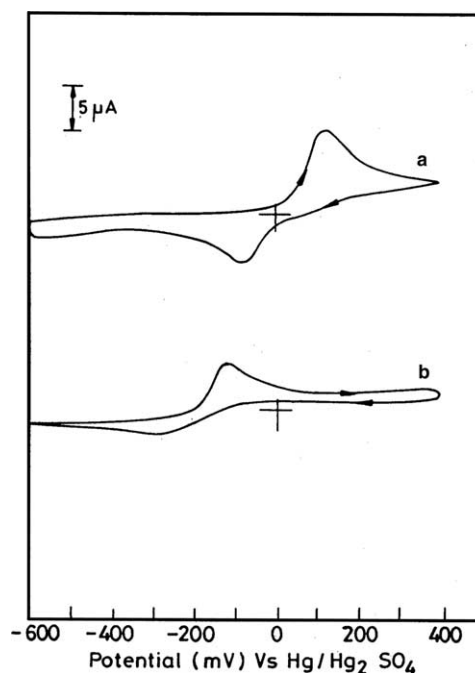
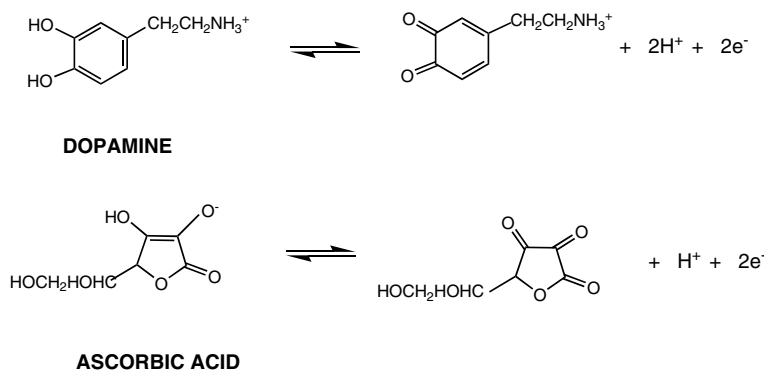
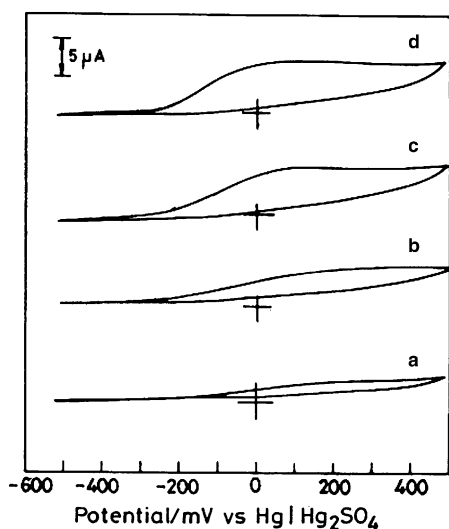
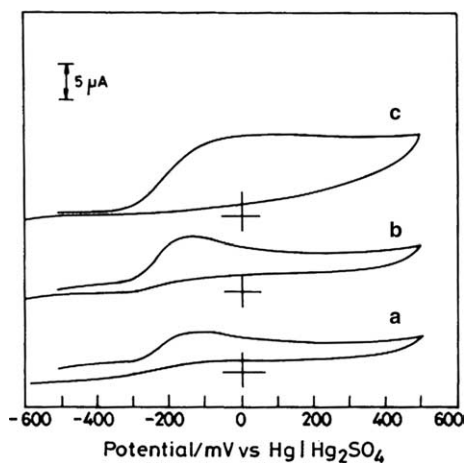


Fig. 1. Cyclic voltammograms showing responses at a bare electrode (a) 1 mM DA and (b) 1 mM AA in phosphate buffer at $v = 50 \text{ mV/s}$.



Scheme 2. Scheme representing the oxidation reaction of DA and AA.

Fig. 2. Cyclic voltammogram showing the response of DA for gradual additions in the case of the Au/DT+MUA electrode: $v = 50$ mV/s. (a) 0.33 mM, (b) 0.66 mM, (c) 0.83 mM and (d) 1.6 mM.Fig. 3. Cyclic voltammogram showing the response of DA for gradual additions to the Au/MUA/Cu²⁺ electrode (a) 0.33 mM, (b) 0.66 mM and (c) 2.0 mM.

oxidation current increases with the gradual addition of DA.

3.2. Selective recognition of DA using monolayers

Fig. 4(A), curve (a), indicates the response of DA (2.1 mM) observed in the presence of the MUA film. DA oxidation occurs as a relatively broad peak at a potential more positive than that observed on the bare electrode. DA, being positively charged, is attracted electrostatically to the negatively charged monolayer of MUA. However electron transfer becomes sluggish as the length of the SAM chain increases, though the long chain thiols are known to form organized films. Therefore DA oxidation occurs at a higher potential with a reduced current and the electrochemical response shows a drawn out wave. Similar behaviour has been observed by other authors [43].

Fig. 4(A), curve (b), describes the changes in the cyclic voltammetric response observed when DA and AA are present together. When the AA concentration is 10 times greater than that of DA, oxidation of AA and DA occur as separate oxidation waves (curve (b), Fig. 4(A)), which is advantageous for the selective recognition, when AA is present in high concentrations along with DA in brain fluids. The two waves observed are at around -0.05 and -0.380 V. The first wave shows the influence of AA on the electrocatalytic oxidation of DA. Therefore the current represented by the first wave increases compared to curve (a). The second wave corresponds to the direct oxidation of AA. The current is higher as the concentration of AA is 10 times that of DA. When AA is present at low concentration there is no change observed in the voltammogram, i.e., the voltammogram represented by curve (a) remains unchanged. This shows that at low concentrations of AA, AA does not interfere with the selective sensing of DA.

Fig. 4(B), curve (a) represents the oxidation of DA (0.33 mM) at the Au/MBT electrode. DA oxidation occurs at a slightly higher value than that observed on a bare electrode as a broad peak. The oxidation current is

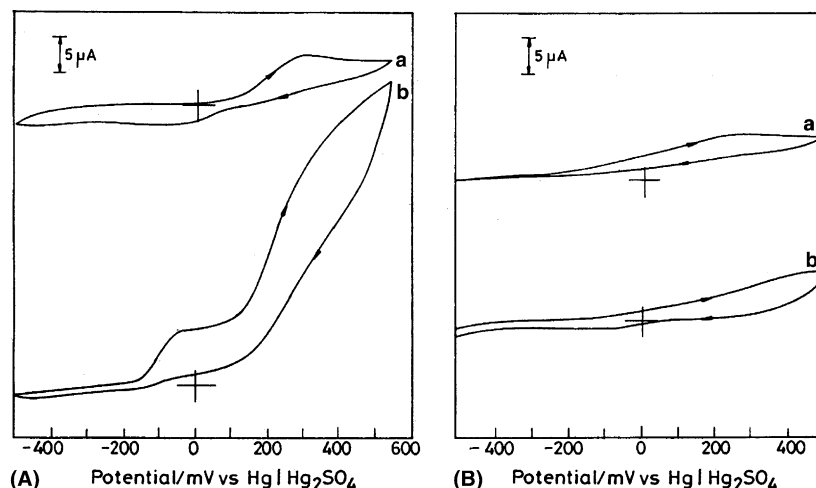


Fig. 4. A: Cyclic voltammogram for the oxidation of DA (2.1 mM) (b) DA (2.1 mM)+AA (21 mM) on the Au/MUA electrode at $v = 50$ mV/s. B: Cyclic voltammogram showing the response of (a) DA (0.33 mM), (b) DA (0.33 mM)+AA (3.3 mM) on the Au/MBT electrode at $v = 50$ mV/s.

reduced due to the distance of the monolayer from the electrode surface, which reduces the electron transfer kinetics. When AA is also present there is no change in the voltammetric response. When the concentration of AA is 10 times the concentration of DA (Fig. 4(B), curve (b)) electrocatalytic oxidation of DA by AA occurs and this is reflected as a current increase. At low concentrations, AA is completely blocked and hence selective sensing of DA is possible. At higher concentrations, the coexistence of AA is felt as an increase in the oxidation current of DA, which represents the electrocatalytic oxidation of DA by AA.

3.3. Selective recognition of DA using mixed monolayers

Fig. 5(A), curve (a) presents the cyclic voltammogram showing the response for 1.6 mM DA at the Au/DT+MUA electrode. When AA alone is present, the film, being negatively charged, will repel the ascorbate

anions; hence no response is observed. DA is oxidized at a potential closer to that of oxidation at the bare electrode. The shape of the response is as observed in the case of Au/MUA indicating a slowing down of the electrochemical kinetics due to the length of the monolayer. When AA is added to the solution, along with DA, we observe that the current increases at a potential close to the oxidation peak which shows the electrocatalysis of DA by AA. The results show that in this film, DA can be selectively sensed at low concentrations of AA. When the concentrations become equal, the selective sensing property is lost (Fig. 5(A), curve (b)). At equal concentrations, DA undergoes electrocatalytic oxidation in the presence of AA.

Fig. 5(B), curve (a), presents the cyclic voltammogram observed for 0.62 mM DA at the Au/(DT+MBT) electrode. It is observed that DA oxidation is observed at a lower positive potential at the Au/(DT+MBT) electrode (−200 mV) compared to that of the bare

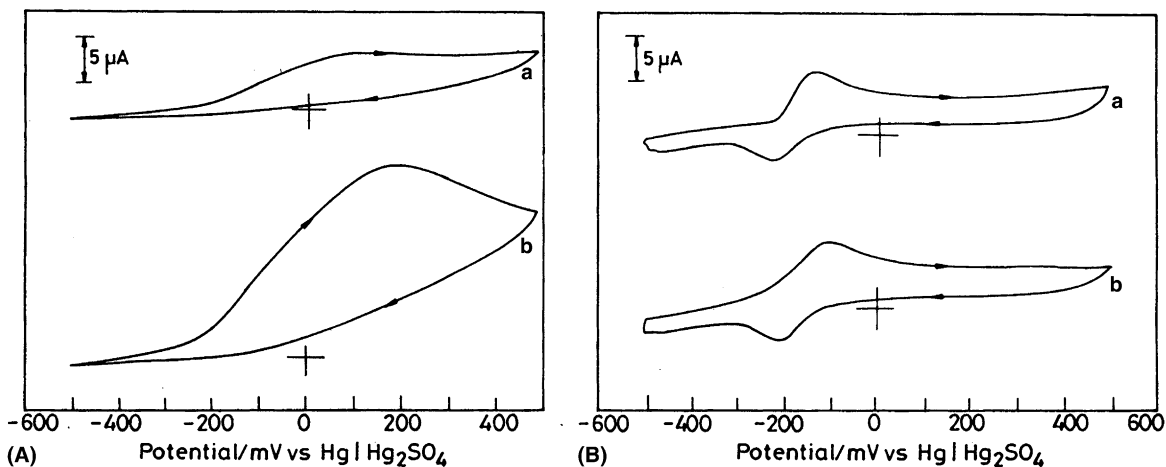


Fig. 5. A: Cyclic voltammogram showing the oxidation of (a) DA (1.6 mM), (b) DA (1.6 mM)+AA (1.6 mM) at the Au/DT+MUA electrode at $v = 50$ mV/s. B: Cyclic voltammogram showing the oxidation of DA (0.62 mM) (b) DA (0.62 mM)+AA (8.3 mM) at the Au/DT+MBT electrode at $v = 50$ mV/s.

electrode. The peak current increases with increase in concentration of DA. The peak response is well defined. No influence of AA was observed in the electrochemical response; i.e., the cyclic voltammograms did not show any change on the addition of AA. Fig. 5(B), curve (b) shows the effect of addition of AA to a concentration ten times that of DA. The influence of AA is seen when the concentration is 20 times greater (not shown in the figure) when the electrocatalytic current starts to appear.

3.4. Bio-inspired recognition

Fig. 6(A), curve (a), present the cyclic voltammogram obtained for the Au/MUA/Cu²⁺ electrode configuration. It is observed from the figure that DA oxidation occurs at a lower overpotential compared to the oxidation at a bare electrode (−150 mV). This indicates that DA is catalytically oxidized at the Au/MUA/Cu²⁺ electrode and the catalytic current increases with increase in concentration of DA. Fig. 6(A), curves (b) and (c), depicts the interference effect of AA. When AA is present at low concentrations there is no effect. When the concentration of AA is increased to 10 times that of DA, two oxidation waves with partial overlap are observed which is again advantageous for selective recognition. One wave is observed around +0.05 V and a broad wave is observed at a higher potential. The first wave has a higher current compared to curve (a), as it contains the contribution due to the electrocatalytic oxidation of DA by AA. The second wave corresponds to the direct oxidation of AA.

Fig. 6(B), curve (a), presents the cyclic voltammograms for the electrode configuration Au/MBT/Cu²⁺.

The DA (0.3 mM) catalytic oxidation occurs at a lower potential of −180 mV. As the concentration of DA increases, the catalytic current also increases and the peak potential shifts to more positive values. On the addition of AA, the current response becomes broader and interference is observed only when the concentration of AA increases to more than 10 times that of DA. When the concentration of AA is 10 times greater, the DA oxidation current increases, which shows the electrocatalysis of DA by AA.

Fig. 7(A), curve (a), depicts the cyclic voltammograms of DA (2 mM) for the electrode configuration Au/(DT+MUA)Cu²⁺. It is clear from the figure that DA is catalytically oxidized at the electrode at low overpotentials (−150 mV) and it is found that the catalytic current increases with an increase in concentration of DA. Only a sample curve is shown in curve (a). When AA is present as an interferent, it is observed there is no effect when the AA concentration is lower than that of DA. When the concentrations of AA and DA are equal, the oxidations of AA and DA occur separately and they are observed as two separate peaks (Fig. 7(A), curve (b)) therefore this electrode configuration is suited for the separation of DA and AA. The wave corresponding to DA (more negative wave of curve (b), Fig. 7(A)) decreases compared to curve (a), Fig. 7(A). The repulsion of AA by the Au/(DT+MUA) layer will be greater compared to the repulsion due to the Au/MUA monolayer, as DT molecules are hydrophobic. Hence the oxidized DA molecules cannot undergo electrocatalytic oxidation by AA, as they do not encounter AA molecules within the proximity of the electrode. Hence there is a decrease in current. When the concentration of

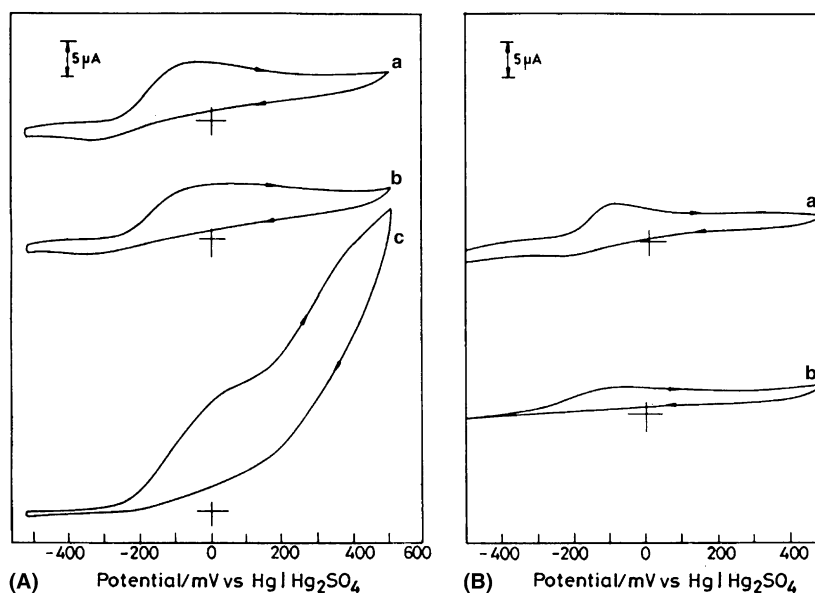


Fig. 6. A: Cyclic voltammogram showing the oxidation of (a) DA (1.6 mM), (b) DA (1.6 mM)+AA (1.6 mM), (c) DA (1.6 mM)+AA (16 mM) on the Au/(MUA) Cu²⁺ electrode at $v = 50$ mV/s. B: Cyclic voltammograms showing the oxidation of (a) DA (0.33 mM), (b) DA (0.33 mM)+AA (3.3 mM) on the Au/(MBT) Cu²⁺ electrode at $v = 50$ mV/s.

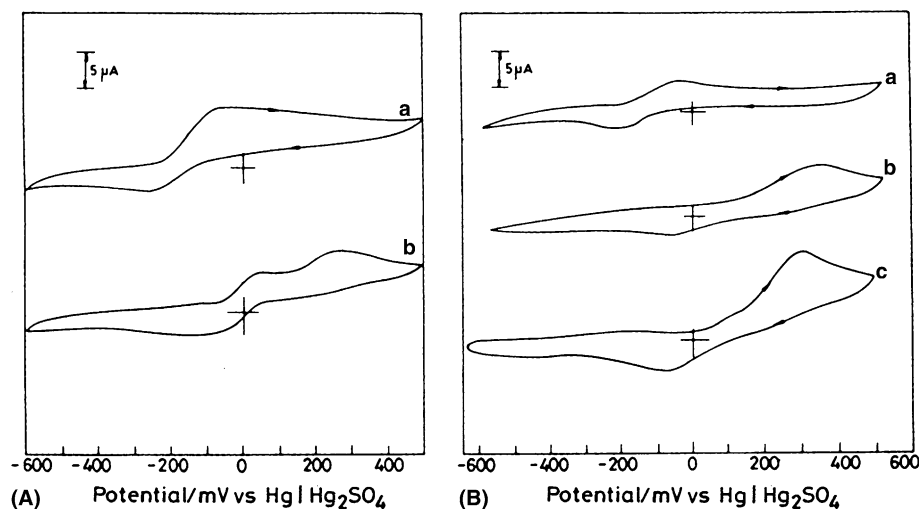


Fig. 7. A: Cyclic voltammograms representing the oxidation of DA (2 mM) (b) DA (2 mM)+AA (2 mM) on the Au/(DT+MUA) Cu²⁺ electrode at $v = 50$ mV/s. B: Cyclic voltammograms showing the oxidation of DA (0.33 mM) (b) DA (0.62 mM), (c) DA (1 mM)+AA (1.6 mM) on the Au/(DT+MBT) Cu²⁺ electrode at $v = 50$ mV/s.

AA is increased tenfold, the DA oxidation current increases. This corresponds to the electrocatalytic oxidation of DA by AA. This is followed by the direct oxidation of AA.

Fig. 7(B); curve (a), presents cyclic voltammograms for Au/(DT+MBT) Cu²⁺ in phosphate buffer for a DA concentration of 0.3 mM. The oxidation occurs at a lower potential of around -60 mV. As the concentration of DA increases, the peak shifts to more positive potentials (Fig. 7(B), curve (b)). The interference effect of AA observed in this film is more pronounced. The current increases by 50% even for equal concentrations of DA and AA (Fig. 7(B), curve (c)).

3.5. Basis of recognition of dopamine vs. ascorbic acid

The thiols used in the present study are MBT, MUA and DT. It has been recently reported by us [54] that MBT monolayers, being negatively charged at neutral pH, can be tuned to discriminate between positively and negatively charged redox species by changing the pH. This concept has been verified with the redox species [Fe(CN)₆]^{3- / 4-} and [Ru(NH₃)₆]^{2+ / 3+}. Typical results obtained are given for the Au/(DT+MUA) configuration in Fig. 8. In the case of Au/MUA films it is observed that the electron transfers due to [Fe(CN)₆]^{4- / 3-} and [Ru(NH₃)₆]^{2+ / 3+} are both blocked at acidic pH, and in phosphate buffer (pH = 7.62), the electron transfer due to ferrocyanide ions is completely blocked while the electron transfer of the species [Ru(NH₃)₆]^{3+ / 2+} occurs with decreased electron transfer kinetics. These observations can be understood from the electrostatic interactions. From these results it can be concluded that, at neutral pH, positively charged species can be selectively recognized and hence the investigations have been made.

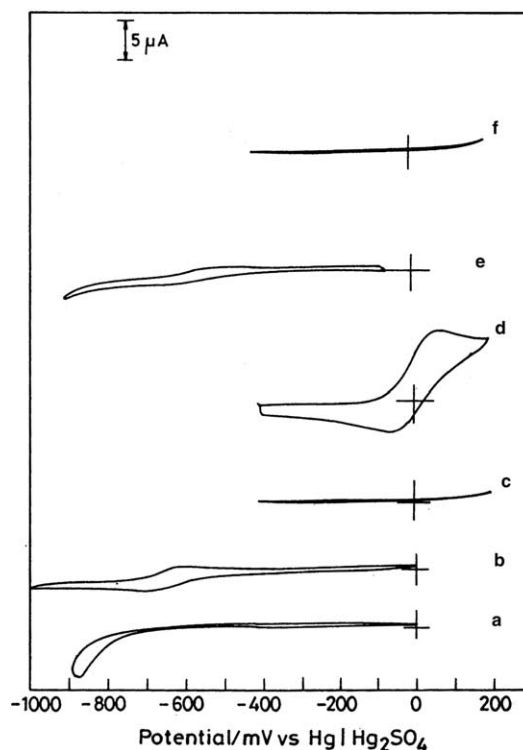


Fig. 8. Cyclic voltammograms showing the response of (a) 1 mM [Ru(NH₃)₆]²⁺ in 0.5 M H₂SO₄, (b) 1 mM [Ru(NH₃)₆]²⁺ in 0.5 M Na₂SO₄, (c) 1 mM [Fe(CN)₆]⁴⁻ in 0.5 M Na₂SO₄, (d) 1 mM [Fe(CN)₆]⁴⁻ in 0.5 M H₂SO₄, (e) 1 mM [Ru(NH₃)₆]²⁺ in phosphate buffer, (f) 1 mM [Fe(CN)₆]⁴⁻ in phosphate buffer on the Au/(DT+MUA) modified electrode; Scan rate = 50 mV/s.

DA oxidation is observed at a slightly higher potential, compared to that at the bare electrode, and the peak observed is irreversible with a current lower than that of a bare electrode in the case of the Au/

MUA and Au/MBT electrode configurations. The reasoning is as follows: MBT and MUA form highly organized monolayers and electron transfer is slowed down as the length of the thiol chain increases. It has been shown that the pK_a value of a carboxylate terminated monolayer shifts from a bulk pK_a value of 4 to a surface pK_a value of 7.5 [55–57] and the pK_a value of MBT is found to be 6.93 at 20 °C. The oxidation is also hindered by Na^+ , which competes with the positively charged DA species to be attracted to COO^- groups [58,59]. This also contributes to the decrease in the electrochemical kinetics in the monolayers. Hence the electrochemical response of DA is observed as a wave/plateau.

3.6. Influence of DT in a mixed monolayer

When the results observed in the case of mixed monolayers are compared, it is found out that the DA oxidation occurs at a lower potential than at the bare electrode and the response is a well defined peak in the case of Au/(DT+MBT) and a broad peak in the case of Au/(DT+MUA). In both cases the currents observed are higher, compared to Au/MBT and Au/MUA (see Table 1). In the case of mixed monolayers, DT molecules stretch out like pillars, and being hydrophobic, they repel the Na^+ ions from attachment to the MBT^- ions. Hence all the anionic groups are free and positively charged DA species can be attached favourably to the anionic species. Hence higher currents are observed in the case of Au/(DT+MBT). In the case of Au/MUA, the length of the MUA chain will be longer than the DT chain. Hence the screening of Na^+ ions will be less. However the presence of DT molecules minimizes the hydrogen bonding between the $-COOH$ groups and therefore more $-COOH$ remains deprotonated than in the free Au/MUA film and hence more current is observed in this case also [59].

Table 1
Potential current characteristics of DA oxidation on the different electrode configurations used in the investigation

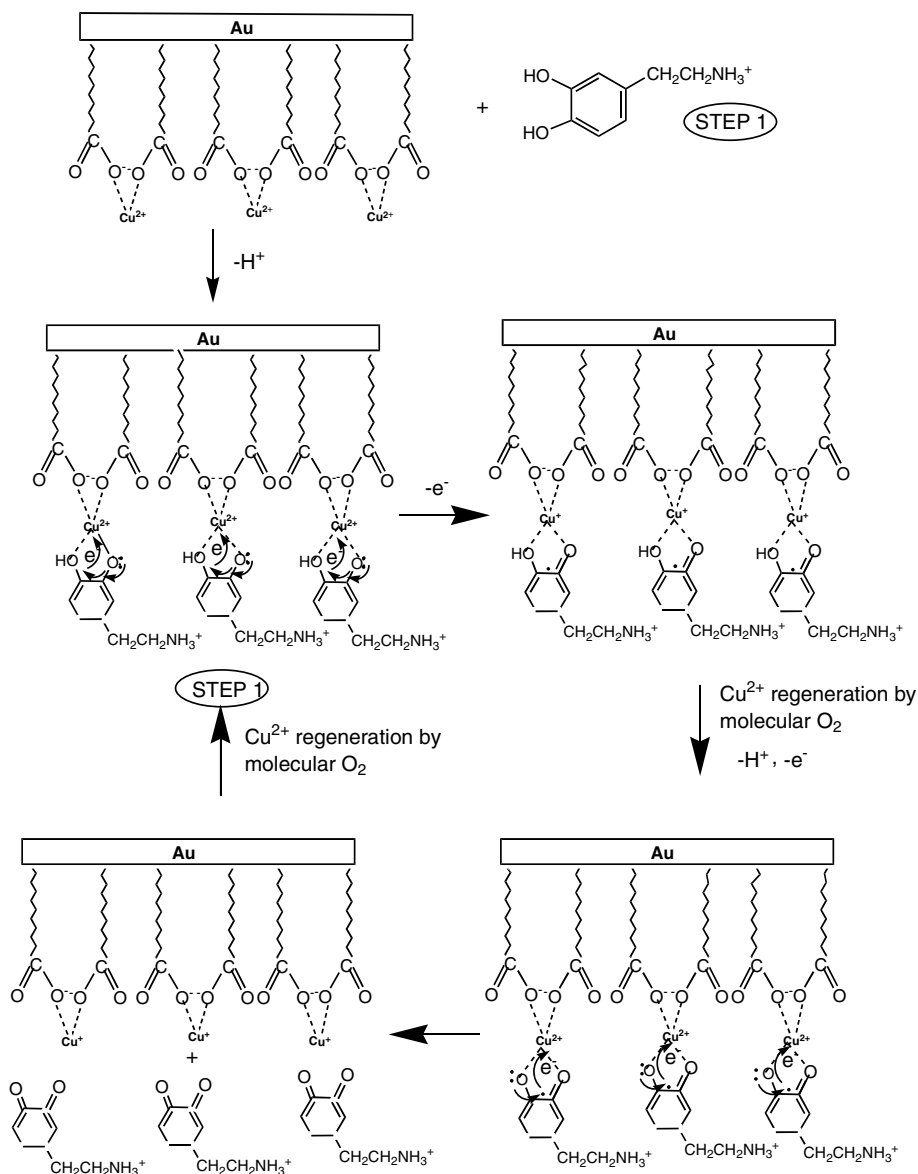
Electrode configuration	[DA] (mM)	I_{DA} (μA)	E_{peak} (mV)	Nature of the peak
Au/MUA	1.42	3.7	280	Broad
Au/DT+MUA	1.426	5.0	50	Broad
Au/MUA/ Cu^{2+}	1.426	5.5	-80	Broad
Au/(DT+MUA) Cu^{2+}	1.426	4.5	-70	Peak
AU/MBT	0.33	1.2	200	Broad
Au/DT+MBT	0.33	3.0	-120	Peak
Au/MBT/ Cu^{2+}	0.33	3.5	-130	Peak
Au/(DT+MBT) Cu^{2+}	0.33	3.5	-100	Peak
Bare Au	1.0	9.0	130	Peak

3.7. Influence of Cu^{2+} ions

In all the configurations with Cu^{2+} , it is observed that DA oxidation occurs at lower potentials compared to the oxidation at the bare electrode since copper catalyses the oxidation. Based on the facts available in the literature [59,60] a tentative mechanism is proposed in Scheme 3. A similar mechanism is proposed where screen-printed Cu electrodes are used to discriminate diphenols from monophenols [60,61]. The influence of Cu^{2+} ions is similar to those observed in biological reactions [1,2]. This mechanism involves the formation of a five membered intermediate of DA with Cu^{2+} , followed by electron transfer and dehydrogenation. The formation of an *o*-quinone derivative with reduced Cu^+ can result in Cu^+ being further reoxidised to Cu^{2+} . The formation of the DA- Cu^{2+} five-membered intermediate is considered to be the factor for selectivity. The mechanism is supported by our observation that the DA oxidation current showed a linear dependence with scan rate (Fig. 9); this indicates a surface thin film process as against a mass transfer controlled process and supports the proposed mechanism. Similar reactions are well established in the solution phase [62].

3.8. Interference due to AA

None of the films used in the present investigation show any response to AA when it is present alone. AA, being negatively charged, will be repelled by the carboxylic acid monolayers at pH = 7.62 when they remain deprotonated. Due to the introduction of DT molecules the repulsion will be greater, as DT is hydrophobic. However, AA molecules oxidize the DA molecules electrocatalytically. The oxidized DA, i.e. DA *o*-quinone is chemically reduced by AA. Hence the oxidation of DA is likely to be altered even though the film is negatively charged and is able to repel ascorbate anions. Further, only if the oxidized DA species encounter AA ions within the proximity of the electrode surface will they be reduced chemically by AA. Therefore, if the diffusion layer thickness is very small, the chances of chemical reduction by AA will be lower. By using of ultramicroelectrodes, this problem of electrocatalysis can be avoided [43]. From our results we see that in the case of Au/MUA, Au/MUA/ Cu^{2+} and Au/(DT+MUA) Cu^{2+} , two well-separated waves are observed when the concentration of AA is 10 times that of DA. The more negative wave is ascribed to DA oxidation and the second wave is ascribed to direct oxidation of AA. In the case of Au/MUA and Au/MUA/ Cu^{2+} electrodes, the electrocatalytic oxidation of DA by AA is reflected as the increase in the current observed for the oxidation of DA. In the case of the Au/(DT+MUA) Cu^{2+} electrode, the current for DA oxidation decreases due to the increased repulsion of AA by the Au/(DT+MUA)

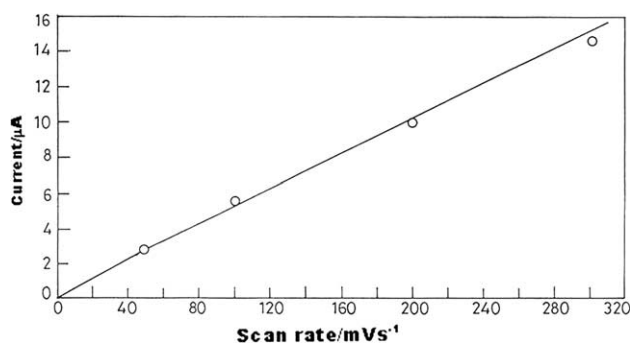


Scheme 3. Proposed reaction mechanism for the bio-inspired oxidation of DA in Au/MUA SAMs [59,60].

monolayer and the absence of electrocatalytic oxidation of DA by AA. Hence these films are best suited for selective recognition. The interference effect of AA de-

pends upon the concentration levels of AA in the solution. The concentration dependence is explained as follows.

The electron transfer kinetics across self assembled monolayers depend on several factors like the length of the alkyl chain, the structural integrity of the monolayer which is determined by the nature of pinholes, defects, etc., and the charge on the terminal groups of the self assembled monolayer. The electron transfer rate decreases as the chain length increases as determined by the Marcus equation. The structural integrity determines the blocking properties of the monolayer. The charge on the terminal groups, which is a function of pH, determines the facility of the kinetics based on electrostatic considerations. MUA and MBT are known to form organized films on gold substrates. The introduction of DT is known to increase the structural

Fig. 9. Linear plot showing the dependence of the DA (0.9 mM) oxidation current with scan rate for the Au/MUA/Cu²⁺ modified electrode.

integrity and hence increases the blocking property of the monolayer and prevents the entry of small electroactive molecules. This blocking property decreases as the concentration increases. Our earlier results on a mixed monolayer of thioctic acid and DT clearly demonstrate this feature [39]. In the present work, we are interested in the electron transfer kinetics of AA and DA on the four films MUA, MBT, DT+MUA and DT+MBT at pH = 7.0. At neutral pH, MUA and MBT are known to be negatively charged. Now the electron transfer across the film is determined by the blocking property or structural integrity and charge on the monolayer. It is observed that in all the four films studied, both the blocking characteristics of the monolayer and the charge on the monolayer prevent the entry of AA into the film. No electrochemical response is observed for AA when it is present alone in the four films. In the case of DA, the response is observed with decreased electrochemical kinetics in the case of MUA and MBT. The length of the chain and the blocking character decrease the electron transfer. Hence the sensing of DA is not at all affected in the presence of low concentrations of AA. When the AA concentration is increased (say by 10 times) the number of negative charges near the monolayer increases at the interface and the monolayer structure is reoriented. In the new orientation, the oxidation of DA and AA are dictated only by electrostatic considerations as observed by Malem and Mandler [43]. Oxidation of DA is shifted favourably to a lower potential. AA oxidation occurs as a separate peak at a higher potential. The observed results fit two types of mechanism. In the case of MUA, MUA/Cu²⁺ and (DT+MUA)Cu²⁺ the observations are similar. As long as the AA concentration is low, the sensing of DA is unaffected by AA. AA is completely blocked by the monolayer. When the concentration of AA increases tenfold, film reorientation takes place and the blocking property decreases. Now the AA molecules are oxidized at a higher potential as the negatively charged monolayer decreases the kinetics. Then selective sensing of DA is possible as two separate peaks are observed.

In the case of the other films, MBT, DT+MBT, (MBT)Cu²⁺ and DT+MUA, as the concentration of AA increases, the monolayer still remains intact and the structural integrity of the monolayer and electrostatic considerations block the AA oxidation. In these films, it is observed that, as the concentration of AA increases, the blocking property of the film is retained. The coexistence of AA is seen in the electrocatalytic oxidation of DA by AA. The electrocatalysis is represented as



However the electrocatalytic oxidation of DA can be avoided by the use of ultramicroelectrodes and selective

sensing can be retained. A linear relationship is observed when the oxidation peak currents of DA are plotted against their respective concentrations. Fig. 10 indicates the application of these films for the analysis of DA, and the sensitivity increases in the case of the films containing chelated Cu²⁺ ions. The analysis has also been performed in the presence of AA (Figs. 11–13). In the case of the Au/MUA electrode, when the concentration of AA is low (0.33 mM) the linear plot is not much altered. When the AA concentration is raised tenfold we

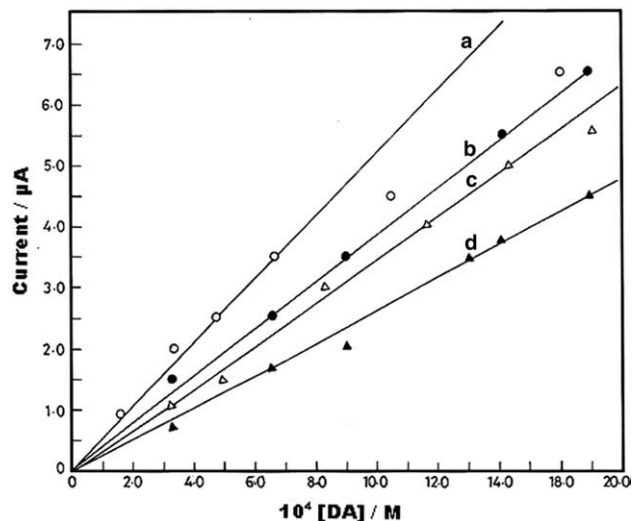


Fig. 10. Graph showing the relationship between peak current (I_p) and concentration of DA on (a) Au/MUA/Cu²⁺, (b) Au/DT+MUA/Cu²⁺, (c) Au/DT+MUA and (d) Au/MUA modified surfaces, $v = 50$ mV/s.

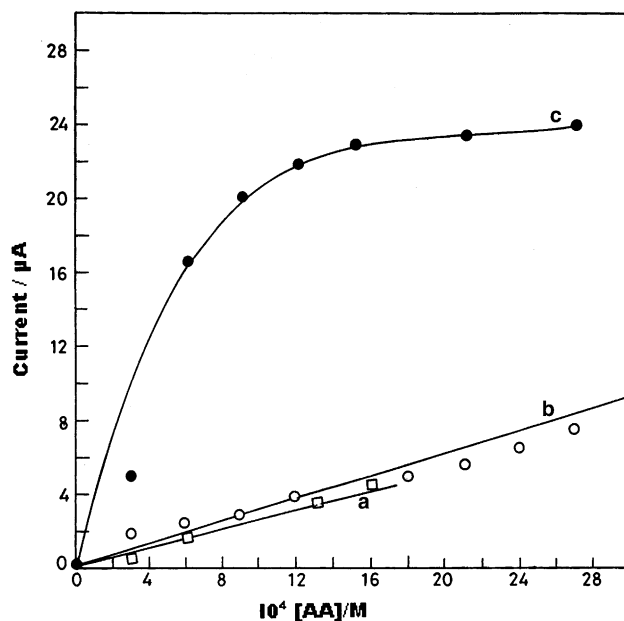


Fig. 11. Graph showing the relationship between the peak current (I_p) and concentration for different additions of DA in the presence of AA on the Au/MUA modified electrode. (a) 0 mM AA, (b) 0.33 mM AA and (c) 3.3 mM AA, $v = 50$ mV/s.

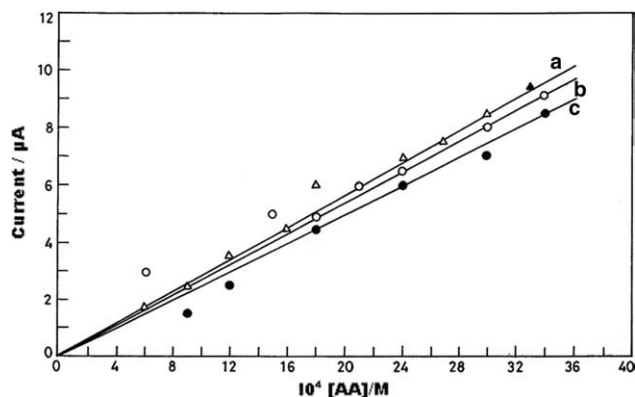


Fig. 12. Graph showing the relationship between peak current (I_p) and concentration for different additions of DA in the presence of AA on the Au/MUA/Cu²⁺ modified electrode (a) 0 mM AA, (b) 0.33 mM AA and (c) 3.3 mM AA, $v = 50$ mV/s.

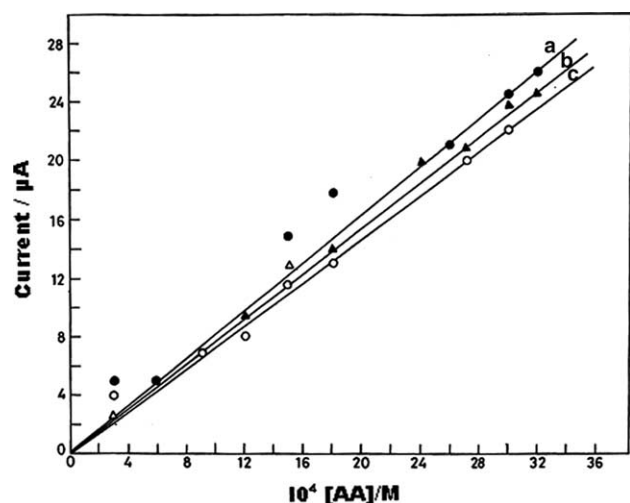


Fig. 13. Graph showing the relationship between the peak current (I_p) and concentration for different additions of DA in the presence of AA on the Au/(DT+MUA)/Cu²⁺ modified electrode. (a) 0 mM AA, (b) 0.33 mM AA and (c) 3.3 mM AA. $v = 50$ mV/s.

obtain a plot as indicated in curve (c) of Fig. 9. Initially there is an increase in current, which represents the electrocatalytic oxidation of DA. After the initial increase, the plot becomes linear for further additions of DA. Hence, even in the presence of AA, linearity is maintained. Figs. 10 and 11 show the results of the analysis carried out in the presence of AA. In the case of Au/MUA/Cu²⁺ and Au/(DT+MUA)Cu²⁺ the plots reveal that the presence of AA does not affect the estimation. We expect to see saturation behaviour in the case of plots showing the variation of peak currents with concentration for the copper derivatised electrodes as we have envisaged a mechanism (Scheme 3) where DA forms a five membered intermediate with Cu²⁺. Fig. 10(a) clearly shows saturation behaviour. In other cases the saturation limit is perhaps not reached and is not seen explicitly. By carrying out the experiments over

a wide range of concentrations, the saturation behaviour can be demonstrated.

4. Conclusions

The results observed have demonstrated the influence of monolayers and mixed monolayers in recognizing DA over AA based on electrostatic considerations. In the case of mixed monolayers, the sensitivity of recognition increases due to the hydrophobicity of DT, the DA oxidation occurs at a lower potential and the currents observed are higher compared to those in the case of monolayers. The presence of Cu²⁺ ions has influenced the recognition property in two ways: (1) by decreasing the overpotential for DA oxidation sufficiently to a negative potential which amounts to a potential gain of around 300 mV, (2) by increasing the current for the oxidation of DA which can be manipulated for detection of the species to low levels of concentration of the order of fractions of mM.

None of the films are found to show any response to AA at neutral pH. AA species, being negatively charged, are repelled from the negatively charged SAMs at neutral pH. However, when AA is present along with DA, most of the films are indifferent to the presence of AA, in the sense that the electrochemical response of DA is not affected by AA for concentrations of AA less than around 10 times the concentration of DA. When the concentration of AA is increased beyond tenfold, the electrocatalytic oxidation of DA is observed. An interesting observation is obtained in the case of the (DT+MUA)/Cu²⁺, Au/MUA and Au/(MUA)Cu²⁺ films. The oxidations of DA and AA are observed as well separated peaks; this is attributed to the reorientation of the film, and the oxidations of DA and AA are dictated by electrostatic considerations only. Hence the concentration of DA can be monitored without the influence of AA. Hence these films are best suited for the selective recognition. In the case of the other films the presence of AA is reflected as the electro catalytic oxidation of DA. The blocking properties of the films are retained at all concentrations of AA. Hence these films are suited for selective sensing only at low concentrations of AA. However by the use of ultramicroelectrodes we can decrease the concentration of oxidized DA in the vicinity of the electrode and hence we can avoid the electrocatalytic effects. This should be a better method for selective sensing and this will be included in our future investigations.

Acknowledgements

The authors wish to express their sincere thanks to the Director, CECRI, for granting permission to carry out the

Ph.D. work of T.M.V, and they would also like to acknowledge the Head, EEC division, CECRI for his encouragement and for providing the laboratory facilities.

References

- [1] P. Gamez, P.G. Aubel, W.L. Dreissen, J. Readijk, *J. Chem. Soc. Rev.* 30 (2001) 376.
- [2] T.D.H. Bugg, G. Lin, *Chem. Commun.* (2001) 941.
- [3] Z. Liu, B. Liu, J. Kong, J. Deng, *Anal. Chem.* 72 (2000) 4707.
- [4] F. Ortega, E. Dominguez, *Biosen. Bioelectron.* 10 (1995) 607.
- [5] J.P. Klinman, *Chem. Rev.* 96 (1996) 2541.
- [6] K. Lerch, in: H. Sigel (Ed.), *Metal Ions in Biological Systems*, Marcel Dekker, New York, 1981, p. 143.
- [7] A.D. Zuberbuhler, in: K.D. Karlin, J. Zubieta (Eds.), *Copper Coordination Chemistry: Biochemical and Inorganic Perspectives*, Academic Press, New York, 1983, p. 237.
- [8] J.C.B. Fernandes, L.T. Kubota, G. de Oliveira Neto, *Anal. Chim. Acta* 385 (1999) 3.
- [9] C. Retna Raj, K. Tokuda, T. Ohsaka, *Bioelectrochemistry* 53 (2001) 183.
- [10] A. Domenech, H. Garcia, M.T. Domenech-Carbo, M.S. Galletero, *Anal. Chem.* 74 (2002) 562.
- [11] C. Retna Raj, T. Ohsaka, *J. Electroanal. Chem.* 496 (2001) 44.
- [12] R.N. Adams, *Anal. Chem.* 48 (1976) 1128A.
- [13] F.G. Gonan, M.J. Buda, *Neuroscience* 14 (1985) 765.
- [14] J.C. Deutsch, J.F. Kolhouse, *Anal. Chem.* 65 (1993) 321.
- [15] J.A. Stamford, J.B. Justice Jr., *Anal. Chem.* 69 (1996) 359A.
- [16] T. Zetterstrom, T. Sharp, C.A. Marsden, U. Ungerstedt, *J. Neurochem.* 41 (1983) 1769.
- [17] P. Capella, B. Ghasemzadeh, K. Mitchell, R.N. Adams, *Electroanalysis* 2 (1990) 175.
- [18] R.M. Wightman, L.J. May, A.C. Michael, *Anal. Chem.* 60 (1988) 769A.
- [19] J.W. Mo, B. Ogoreve, *Anal. Chem.* 73 (2001) 1196.
- [20] T.F. Kang, G.L. Shen, R.Q. Yu, *Anal. Chim. Acta* 356 (1997) 245.
- [21] C. Husch, R. Bravo, A.J. Jaramilo, A. Brajter-Toth, *Anal. Chim. Acta* 349 (1997) 67.
- [22] Z. Gao, D. Yap, Y. Zhang, *Anal. Sci.* (1998) 1059.
- [23] R.D. O' Neill, *Analyst* 119 (1994) 767.
- [24] M.A. Dayton, A.G. Ewing, R.M. Wightman, *Anal. Chem.* 52 (1980) 2392.
- [25] J.B. Justice Jr., A. Jaramillo, *J. Electrochem. Soc.* 131 (1984) 106C.
- [26] H. Zhao, Y. Zhang, Z. Yuan, *Electroanalysis* 14 (2002) 1031.
- [27] A. Ciszewski, G. Milczarek, *Anal. Chem.* 71 (1999) 1055.
- [28] J. Wang, A. Walcarius, *J. Electroanal. Chem.* 407 (1996) 183.
- [29] J.M. Zen, P. Chen, *Anal. Chem.* 69 (1997) 5087.
- [30] A.M. Farrington, J.M. Slater, *Electroanalysis* 9 (1997) 843.
- [31] F. Gonon, M. Buda, R. Cespuoglio, M. Jouvet, J.F. Pujol, *Nature* 286 (1980) 902.
- [32] J.M. Cooper, P.L. Foreman, A. Glidle, T.W. Ling, D.J. Pritchard, *J. Electroanal. Chem.* 388 (1995) 143.
- [33] B. Duong, R. Arechabaleta, N.J. Tao, *J. Electroanal. Chem.* 447 (1998) 63.
- [34] S. Berchmans, V. Yegnaraman, G. Prabhakara Rao, *Proc. Indian Acad. Sci. (Chem. Sci.)* 109 (1997) 277.
- [35] S. Berchmans, V. Yegnaraman, N. Sandhyarani, K.V.G.K. Murty, T. Pradeep, *J. Electroanal. Chem.* 170 (1999) 468.
- [36] S. Bharathi, V. Yegnaraman, G. Prabhakara Rao, *Langmuir* 9 (1993) 1614.
- [37] S. Bharathi, V. Yegnaraman, G. Prabhakara Rao, *Langmuir* 11 (1995) 666.
- [38] S. Berchmans, S. Arivukkodi, V. Yegnaraman, *Electrochem. Commun.* 2 (2000) 226.
- [39] S. Berchmans, C. Ramalechume, V. Lakshmi, V. Yegnaraman, *J. Mater. Chem.* 12 (2002) 2538.
- [40] S. Berchmans, V. Yegnaraman, G. Prabhakara Rao, *J. Solid State Electrochem.* 3 (1998) 52.
- [41] R.C. Weast (Ed.), *CRC Handbook of Chemistry and Physics*, 60th ed., CRC Press, Boca Raton, FL, 1979-1980.
- [42] R.A. Saraceno, J.G. Pack, A.G. Ewing, *J. Electroanal. Chem.* 197 (1986) 265.
- [43] F. Malem, D. Mandler, *Anal. Chem.* 65 (1993) 37.
- [44] M.R. Khan, S.B. Khoo, *Analyst* 126 (2001) 2172.
- [45] R. Woods, G.A. Hope, K. Watling, *J. Appl. Electrochem.* 30 (2001) 209.
- [46] J. Wang, B. Zong, C. Fang, X. Zhou, *Anal. Sci.* 16 (2000) 457.
- [47] A.E. Mantell, R.M. Smith, in: *Critical Stability Constants*, vol. 3, Plenum, New York, 1997, p. 313.
- [48] J.L. Kice, N. Elliot, N. Marvell, *Modern Principles Of Organic Chemistry – An Introduction*, Macmillan, New York, 1965, p. 360.
- [49] J. Lipkowski, L. Stolberg, in: J. Lipkowski, P.N. Ross (Eds.), *Adsorption of Molecules at Metal Electrodes*, VCH, New York, 1992, p. 268.
- [50] N. Sandhyarani, G. Skanth, S. Berchmans, V. Yegnaraman, T. Pradeep, *J. Colloid Interface Sci.* 209 (1999) 154.
- [51] C.M. Whelan, M.R. Smyth, C.J. Barnes, *J. Electroanal. Chem.* 441 (1998) 109.
- [52] G. Xue, Y. Lu, *Langmuir* 10 (1994) 967.
- [53] J. Luo, N. Kariuki, L. Han, M.M. Maye, L.W. Moussa, S.R. Kowaleski, F.L. Kirk, M. Hepel, C.J. Zhong, *J. Phys. Chem. B* 106 (2002) 9313.
- [54] T.M. Vergeheese, S. Berchmans, *Seventh International Symposium on Advances in Electrochemical Science and Technology (ISA-EST-VII) Chennai, India, 2002 November 27–29*, A. No 1.26 and 1.27, p. 35.
- [55] S.R. Holmes-Farley, R.H. Reamey, T.J. McCarthy, J. Deutch, G.M. Whitesides, *Langmuir* 1 (1985) 725.
- [56] C.D. Bain, G.M. Whitesides, *Langmuir* 5 (1989) 1370.
- [57] S.E. Creager, J. Clarke, *Langmuir* 10 (1994) 3675.
- [58] T. Moeller, *Inorganic Chemistry*, John Wiley and Sons, New York, 1982.
- [59] A. Dalmia, C.C. Liu, R.F. Savinell, *J. Electroanal. Chem.* 430 (1997) 205.
- [60] L. Rover Jr., J.C.B. Fernandes, G. de Oliveira Neto, L.T. Kubota, *J. Electroanal. Chem.* 481 (2000) 34.
- [61] J.M. Zen, H.H. Cheng, A.S. Kumar, *Anal. Chem.* 74 (2002) 1202.
- [62] M.M. Rogic, T.R. Demmin, *J. Am. Chem. Soc.* 100 (1978) 5472.